Vented-Box Loudspeaker Systems
Part I: Small-Signal Analysis

RICHARD H. SMALL

School of Electrical Engineering, The University of Sydney, Sydney, N.S.W. 2006, Australia

The low-frequency performance of a vented-box loudspeaker system is directly related to a small number of easily measured system parameters. This system is a fourth-order (24-dB per octave cutoff) high-pass filter which can be adjusted to have a wide variety of response characteristics. Enclosure losses have a significant effect on system performance and should be taken into account when assessing or adjusting vented-box systems. The efficiency of a vented-box loudspeaker system is shown to be quantitatively related to system frequency response, internal losses, and enclosure size.

LIST OF IMPORTANT SYMBOLS

f_B	Resonance frequency of vented enclosure
f_H	Frequency of upper voice-coil impedance peak
f_L	Frequency of lower voice-coil impedance peak
f_M	Frequency of minimum voice-coil impedance between f_L and f_H
f_S	Resonance frequency of driver
f_{SB}	Resonance frequency of driver mounted in enclosure
f_3	Half-power (-3 dB) frequency of loudspeaker system response
$G(s)$	Response function
h	System tuning ratio, $= f_B/f_S$
k_P	Power rating constant
k_η	Efficiency constant
P_{AR}	Displacement-limited acoustic power rating
P_{ER}	Displacement-limited electrical power rating
$P_{E(\max)}$	Thermally limited maximum input power
Q_A	Enclosure Q at f_B resulting from absorption losses
Q_B	Total enclosure Q at f_B resulting from all enclosure and vent losses
Q_L	Enclosure Q at f_B resulting from leakage losses
Q_P	Enclosure Q at f_B resulting from vent frictional losses
Q_{ES}	Driver Q at f_S considering electrical resistance R_E only
Q_{MS}	Driver Q at f_S considering driver nonelectrical losses only
Q_{TS}	Total driver Q at f_S resulting from all driver resistances
Q_T	Total driver Q at f_S resulting from all system resistances
R_E	Dc resistance of driver voice coil
V_{AS}	Volume of air having same acoustic compliance as driver suspension
V_B	Net internal volume of enclosure
V_D	Peak displacement volume of driver diaphragm
$x_{\max}$	Peak linear displacement of driver diaphragm
$X(s)$	Displacement function
α	System compliance ratio, $= V_{AS}/V_B$
η_0	Reference efficiency.

1. INTRODUCTION

Historical Background

The concept of the vented loudspeaker enclosure was introduced by Thuras in a U.S. patent application of 1930 [1]. The principle of operation of the system is described in considerable detail in this document which recognizes the interaction of diaphragm and vent radiation, presents several possible methods of construction, and includes a polynomial expression for the frequency-dependent behavior.

In 1952 Locanthi [2] provided the first means of calculating the exact magnitude of diaphragm–vent interaction and introduced the use of electrical analog networks to study the performance of vented-box systems.

In 1954 Beranek [3, ch. 8] derived a polynomial expression for the response of a vented-box system which was much simpler than Thuras' expression. Beranek ignored diaphragm–vent interaction and gave results for the relative response at three discrete frequencies, taking into account the system losses and including the exact effects of the variation with frequency of the radiation load resistance.

The first successful attempt to penetrate both the analysis and design of the vented-box system was published by van Leeuwen in 1956 [4]. This paper examines diaphragm–vent interaction and the effects of both parallel and series resistance in the vent. The analysis gives polynomial expressions for the frequency response and indicates the system poles and their relationship to the system transient response. Van Leeuwen studied the voice-coil impedance and determined accurate methods of calculating the driver and system parameters (and their nonlinearities) from measurement of this impedance. Also, he presented system design methods for obtaining a response characteristic of the equal-ripple (Chebyshev) type and illustrated the use of analog circuits to study the voice-coil impedance and the steady-state and transient response of the system. Unfortunately, this paper was published only in Dutch and was not widely read.

In 1959 de Boer [5], incorporating the diaphragm–vent interaction analysis of Lyon [6], showed clearly that the problem of vented-box system design was a problem of high-pass filter synthesis. Working independently, Novak [7] published in the same year an analysis which provided a simplified transfer function, methods for determining the driver and system parameters from voice-coil impedance measurements, and a clear indication of the amount of driver damping required for flat response.

A year later, Keibs [8] published a penetrating analysis which provided specific quantitative design criteria for the conditions of maximally flat amplitude response and optimum (as defined) transient response.

In 1961 two papers published almost simultaneously but independently brought the understanding of vented-box systems in English-language publications up to and beyond the level attained by van Leeuwen. First de Boer, who had in fact read van Leeuwen's paper, extended his own earlier approach using network-synthesis techniques to provide a much more lucid result. De Boer's paper [9] provides design solutions for both Butterworth and Chebyshev responses. While de Boer's analytical approach can only be described as elegant, the paper is mainly theoretical and does not provide any detailed guide to physical realization.

Later in 1961, Thiele [10], working with the simplified model established by Novak [7], published an analysis which included exhaustive treatment of the practical matters of realization. It is interesting that Thiele's paper, written completely independently of de Boer's, follows almost exactly the analysis–approximation–synthesis procedure outlined by de Boer in his introduction. Thiele's paper provides a much wider range of "optimum" responses than any previous paper, treats the amplifier as an integral part of the system, and provides simple and accurate methods of determining both driver and system parameters through measurement of the voice-coil impedance. It is probably fair to say that Thiele's paper was the first to provide an essentially complete, comprehensive, and practical understanding of vented-box systems on a quantitative level.

While both de Boer and Thiele published in English, neither paper appears to have been widely read (or understood) at the time of publication. Only after 10 years has Thiele's paper been recognized as a classic and republished for a wider audience.

In 1969 Nomura [11] pointed out that enclosure losses often contribute substantial response errors. Nomura's paper provides design solutions for Chebyshev, "degenerated" Chebyshev, and Butterworth responses which include the effects of absorption losses in the enclosure.

A very recent paper by Benson [32] contains the most complete small-signal treatment of vented-box systems yet available and covers several interesting topics not discussed here. A number of footnotes have been added to the text of this paper to make reference to the improved understanding or techniques developed by Benson or to indicate areas in which further information may be gained from his paper.

Technical Background

The vented-box loudspeaker system is a direct-radiator system using an enclosure which has two apertures. One aperture accommodates a driver. The other, called a vent or port, allows air to move in and out of the enclosure in response to the pressure variations within the enclosure.

The vent may be formed as a simple aperture in the enclosure wall or as a tunnel or duct which extends inward from the aperture. In either case, the behavior of the air in the vent is reactive, i.e., it acts as an inertial mass. At low frequencies, the motion of air in the vent contributes substantially to the total volume velocity crossing the enclosure boundaries and therefore to the system output [12].

The analysis of vented-box systems in this paper is essentially an extension of Thiele's approach [10]; it follows the organization of [12] which is in fact a generalized description of Thiele's methods. The principal extensions to Thiele's work include treatment of efficiency–response relationships and large-signal behavior, evaluation of diaphragm–vent interaction, assessment of the magnitude and effects of normal enclosure losses, and calculation of alignment data for systems having such losses. The treatment of enclosure losses is different from that of Nomura [11] because the absorption losses considered by Nomura are found to contribute only a portion of the losses present in practical enclosures.

Some of the analytical results presented in this paper are either obtained or illustrated with the help of an analog circuit simulator similar to that used by Locanthi [2]. Such a simulator is an invaluable aid in the analysis and design of loudspeaker systems because it provides rapid assessment of both time-domain and frequencydomain performance. It is particularly useful in investigating the effects of losses, component tolerances, system misalignment, etc., on response, diaphragm excursion, and voice-coil impedance. It provides results in a fraction of the time that would be required using normal computational methods.

The analytical relationships developed in this paper show that the important performance characteristics of vented-box systems are directly related to a number of basic and easily measured system parameters. Both the assessment and the specification of performance at low frequencies for such systems are therefore relatively simple tasks.

In Parts I and II it is shown that these analytical relationships impose definite quantitative limitations on both small-signal and large-signal performance of vented-box systems and indicate the extent to which the important performance characteristics may be traded off against one another.

In Part III these relationships lead to a method of synthesis (system design) which is free of trial-and-error procedures. This method starts with the desired performance characteristics, checks these for realizability, and results in complete specification of the required system components.

The appendices of the paper are included in Part IV.

2. BASIC ANALYSIS

The impedance-type acoustical analogous circuit of a vented-box loudspeaker system is presented in Fig. 1. This circuit is derived from the generalized circuit of [12, Fig. 2] by short-circuiting the port compliance element. In Fig. 1, the symbols are defined as follows:

- e_g Open-circuit output voltage of source or amplifier
- B Magnetic flux density in driver air gap
- l Length of voice-coil conductor in magnetic field of air gap
- S_D Effective projected surface area of driver diaphragm
- R_g Output resistance of source or amplifier
- R_E Dc resistance of driver voice coil
- C_{AS} Acoustic compliance of driver suspension
- M_{AS} Acoustic mass of driver diaphragm assembly including voice coil and air load
- R_{AS} Acoustic resistance of driver suspension losses
- C_{AB} Acoustic compliance of air in enclosure
- R_{AB} Acoustic resistance of enclosure losses caused by internal energy absorption
- R_{AL} Acoustic resistance of enclosure losses caused by leakage
- M_{AP} Acoustic mass of port or vent including air load
- R_{AP} Acoustic resistance of port or vent losses
- U_D Volume velocity of driver diaphragm
- U_P Volume velocity of port or vent
- U_L Volume velocity of enclosure leakage
- U_B Volume velocity entering enclosure
- U_0 Total volume velocity leaving enclosure boundaries.

This circuit may be simplified to that of Fig. 2 by combining the series resistances in the driver branch to form a single acoustic resistance R_{AT}, where

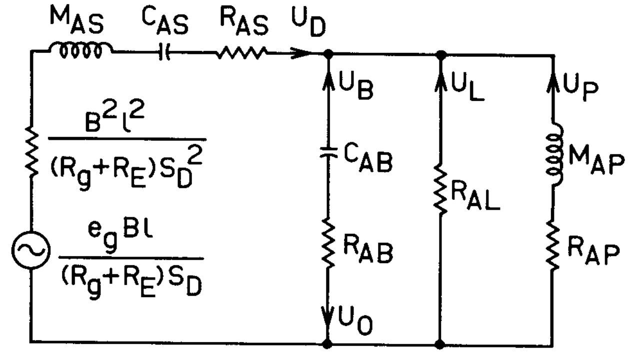

Fig. 1. Acoustical analogous circuit of vented-box loudspeaker system.

$$R_{AT} = R_{AS} + \frac{B^2l^2}{(R_g + R_E)S_D^2} \tag{1}$$

and by defining

$$p_g = \frac{e_gBl}{(R_g + R_E)S_D} \tag{2}$$

as the value of the Thevenin acoustic pressure generator at the left of the circuit. Finally, R_{AB} and R_{AP} are neglected because, as described in the next section, their effects can normally be accounted for by a suitable adjustment to the value of R_{AL}.

By comparison, the circuit used by Novak [7] and Thiele [10] is obtained from that of Fig. 2 by removing the resistance R_{AL}.

The electrical equivalent circuit of the vented-box system is formed by taking the dual of Fig. 1 and converting all impedance elements to their electrical equivalents by the relationship

$$Z_E = B^2l^2/(Z_AS_D^2) \tag{3}$$

where Z_A is the impedance of an element in the impedance-type acoustical analogous circuit and Z_E is the impedance of the corresponding element in the electrical equivalent circuit. A simplified electrical equivalent circuit corresponding to Fig. 2 is shown in Fig. 3. In this circuit,

- C_{MES} Corresponds to driver mass M_{AS}
- L_{CES} Corresponds to driver suspension compliance C_{AS}
- R_{ES} Corresponds to driver suspension resistance R_{AS}
- L_{CEB} Corresponds to enclosure compliance C_{AB}
- R_{EL} Corresponds to enclosure leakage resistance R_{AL}
- C_{MEP} Corresponds to vent mass M_{AP}.

The circuits presented above are valid only for frequencies within the piston range of the system driver; the element values are assumed to be independent of frequency within this range.

As discussed in [12], the effects of the voice-coil inductance and the resistance of the radiation load are neglected. The effect of external acoustic interaction between driver diaphragm and vent [2], [6] has also been neglected. The reasons for this are given later in the paper.

The analysis of the system and the interpretation of its describing functions are simplified by defining a num-

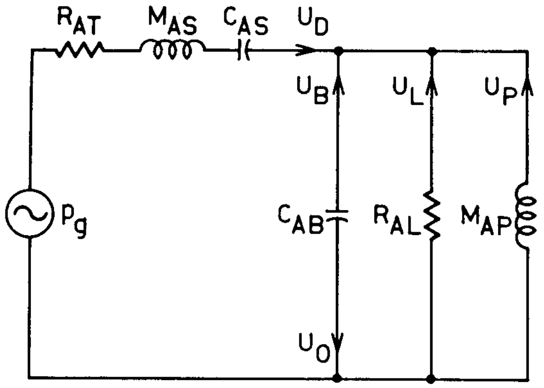

Fig. 2. Simplified acoustical analogous circuit of vented-box loudspeaker system.

ber of component and system parameters. For the enclosure, these are

$$T_B^2 = 1/\omega_B^2 = C_{AB}M_{AP} = C_{MEP}L_{CEB} \quad (4)$$

$$Q_L = \omega_B C_{AB} R_{AL} = 1/(\omega_B C_{MEP} R_{EL}). \quad (5)$$

From Figs. 2 and 3 it can be seen that $\omega_B = 2\pi f_B$ is the resonance frequency of the enclosure–vent circuit, and that Q_L represents the Q of this resonant circuit at ω_B resulting from the leakage losses.

Similarly, the system driver is described by the driver parameters introduced in [12]. These are

$$T_S^2 = 1/\omega_S^2 = C_{AS}M_{AS} = C_{MES}L_{CES} \quad (6)$$

$$Q_{MS} = \omega_S C_{MES} R_{ES} = 1/(\omega_S C_{AS} R_{AS}) \quad (7)$$

$$Q_{ES} = \omega_S C_{MES} R_E = \omega_S R_E M_{AS} S_D^2/(B^2 l^2) \quad (8)$$

$$V_{AS} = \rho_0 c^2 C_{AS}. \quad (9)$$

In Eq. (9) ρ_0 is the density of air (1.18 kg/m^3) and c is the velocity of sound in air (345 m/s). In this paper it is assumed that the values of the first three parameters apply to the driver when the diaphragm air-load mass is that for the driver mounted in the system enclosure [3, pp. 216-217].

The interaction of the source, driver, and enclosure give rise to further system parameters. These are the system compliance ratio α, given by

$$\alpha = C_{AS}/C_{AB} = L_{CES}/L_{CEB} \quad (10)$$

the system tuning ratio h, given by

$$h = f_B/f_S = \omega_B/\omega_S = T_S/T_B \quad (11)$$

and the total Q of the driver connected to the source Q_T, given by

$$Q_T = 1/(\omega_S C_{AS} R_{AT}). \quad (12)$$

Following the method of [12], analysis of the circuits of Figs. 2 and 3 and substitution of the parameters defined above yields the system response function

$$G(s) = \frac{s^4 T_B^2 T_S^2}{s^4 T_B^2 T_S^2 + s^3(T_B^2 T_S/Q_T + T_B T_S^2/Q_L) + s^2[(\alpha+1)T_B^2 + T_B T_S/Q_L Q_T + T_S^2] + s(T_B/Q_L + T_S/Q_T) + 1} \quad (13)$$

where $s = \sigma + j\omega$ is the complex frequency variable, the diaphragm displacement function

$$X(s) = \frac{s^2 T_B^2 + s T_B/Q_L + 1}{D(s)} \quad (14)$$

where $D(s)$ is the denominator of Eq. (13), the displacement constant

$$k_x = 1 \quad (15)$$

and the voice-coil impedance function

$$Z_{VC}(s) = R_E + R_{ES}\frac{s(T_S/Q_{MS})(s^2 T_B^2 + s T_B/Q_L + 1)}{D'(s)} \quad (16)$$

where $D'(s)$ is the denominator of Eq. (13) but with Q_T wherever it appears replaced by Q_{MS}.

3. ENCLOSURE LOSSES

In any vented-box loudspeaker system, three kinds of enclosure losses are present: absorption losses, leakage losses, and vent losses. These losses correpond to the resistances R_{AB}, R_{AL}, and R_{AP} in Fig. 1. The magnitude of each of these losses may be established by defining a value of Q for the enclosure-vent resonant circuit at f_B, considering each loss one at a time. Thus for the leakage losses,

$$Q_L = \omega_B C_{AB} R_{AL} \quad (5)$$

for the absorption losses,

$$Q_A = 1/(\omega_B C_{AB} R_{AB}) \quad (17)$$

and for the vent losses

$$Q_P = 1/(\omega_B C_{AB} R_{AP}). \quad (18)$$

The total Q of the enclosure–vent circuit at f_B is then defined as Q_B, where

$$1/Q_B = 1/Q_L + 1/Q_A + 1/Q_P. \quad (19)$$

It is this Q_B that is measured in a practical system using the method of Thiele described in [10, sec. 14] and in Section 7 (Part II) of this paper.

This paper deals only with systems in which enclosure losses are kept to a practical minimum. Systems making use of deliberately enlarged enclosure losses (e.g., large leaks, resistively damped vents, heavily damped or filled enclosures) will be treated in a later paper.

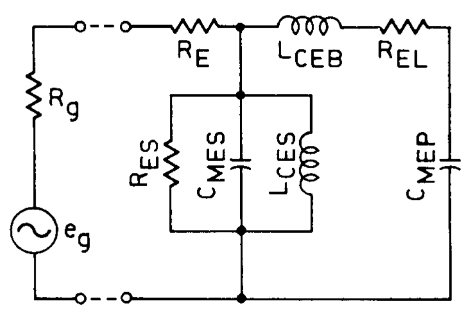

Fig. 3. Simplified electrical equivalent circuit of vented-box loudspeaker system.

Assessment of the contribution of enclosure losses to system performance requires meaningful answers to two questions. First, what is the effect of each kind of loss on system performance? Second, what are the typical magnitudes of the three kinds of losses in practical enclosures?

The answer to the first question has been obtained by constructing the circuit analog of a vented-box system and observing the change in response as a "lossless" enclosure is provided successively with individual leakage, absorption, and vent losses corresponding to a given value of Q. The results for the fourth-order Butterworth (B4) alignment given by Thiele in [10, Table I] are shown in Fig. 4 for Q values of 5. As indicated by Thiele [10, eq. (90)], the maximum response loss occurs at f_B and to a very close approximation depends only on Q_B and not on the actual nature of the loss or losses present. Above f_B absorption losses have the greatest effect and vent losses the least effect on response, while below f_B the relative effects are reversed. The effect of leakage losses is intermediate both above and below f_B. The relative effects are the same for other alignments given in [10], except that, as stated by Thiele, the response loss for a given value of Q_B is greater for alignments having a lower compliance ratio and smaller for alignments having a higher compliance ratio.

The second question has troubled a great many authors because measured losses tend to be higher than the values predicted from theory. Both Beranek [3, p. 257] and Thiele [10, footnote to sec. 14] suspected that absorption losses were to blame for their low measured values of Q_B, and Nomura's paper [11] is based on the assumption that these losses are dominant. Van Leeuwen found that neither lining nor bracing of the enclosure affected his loss measurements [4] and concluded that absorption losses were not significant. He suspected that his extra losses arose in the vent and could be explained only by assuming an increased value for the coefficient of viscosity of air—about 30 times larger than the normally accepted value.

It is possible to determine the magnitude of each kind of loss in practical systems by an extension of Thiele's measurement method as described in Appendix 3. From measurements of this type on a number of commercial and experimental systems, the following was found.

1) Losses in unobstructed vents are usually about the same as or a little greater than the values calculated from viscous theory [10, eq. (7)]. Typical values of Q_P for unobstructed vents are in the range of 50–100. If the vent is obstructed by grill cloth or lining materials, the value of Q_P can fall considerably, but with reasonable care in design need not fall below 20.

2) Absorption losses in unlined enclosures are quite small, giving Q_A values of 100 or more. Typical lining materials placed on the enclosures walls where air particle velocity is low do not extract very much energy [13, p. 383] but can reduce Q_A to a range of 30–80. Very thick linings or damping partitions reduce Q_A even further.

3) Leakage losses are usually the most significant, giving Q_L values of between 5 and 20.

The last result is surprising, because the enclosures tested were well built and appeared to be quite leak-free. In fact, some of the more serious leaks were traced to the drivers. These leaks were caused by imperfect gasket seals and/or by leakage of air through a porous dust cap and past the voice coil. However, the few systems having drivers with solid dust caps and perfect gaskets still had dominant measured leakage losses.

Confidence in the measurement method, based on its ability to detect with reasonable accuracy the deliberate introduction of small additional enclosure losses, leads to the conclusion that the measured leakage in apparently leak-free systems is not an error of measurement but an indication that the actual losses in the system enclosure are not constant with frequency as assumed in the method of measurement (Appendix 3).

The analog circuit simulator has proved to be an invaluable aid in reaching and supporting this conclusion and also in establishing the practical meaning and usefulness of the total-loss measurement. First, it has shown that vent losses which increase with frequency and absorption losses which decrease with frequency do indeed appear in the measurement results as apparent leakage. Second, it has shown that where such frequency-varying losses are present, the system response is predicted with extremely high accuracy from the measured values of Q_A, Q_L, and Q_P as defined.

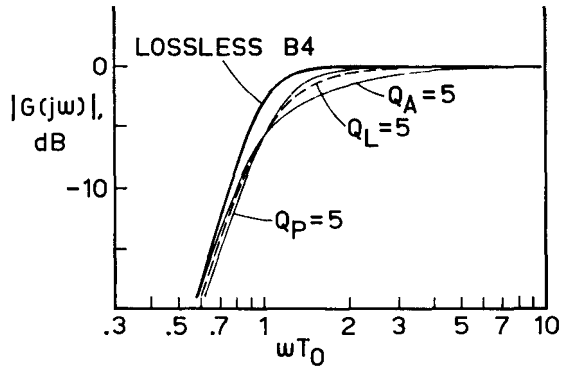

Fig. 4. Effects of enclosure-circuit losses on response of a lossless B4-aligned vented-box loudspeaker system (from simulator).

Finally, and not surprisingly in view of Fig. 4, it has shown that approximately equal values of Q_A and Q_P in the range of values normally measured in practical enclosures have a combined effect on system response which is effectively indistinguishable from the same total value of Q_L.

The above findings lead to the conclusion that even where *actual* leakage is not dominant, the enclosure losses present in a normal vented-box system may be adequately approximated, for purposes of evaluation or design, by a single frequency-invariant leakage resistance. The value of this equivalent leakage resistance is such that the corresponding value of Q_L is equal to the total Q_B that would be measured in the real system by Thiele's method. This approximation is reflected in Figs. 2 and 3 and in the system describing functions Eqs. (13), (14), and (16).

4. RESPONSE

Response Function

The response function of the vented-box system is given by Eq. (13). This is a fourth-order (24-dB per

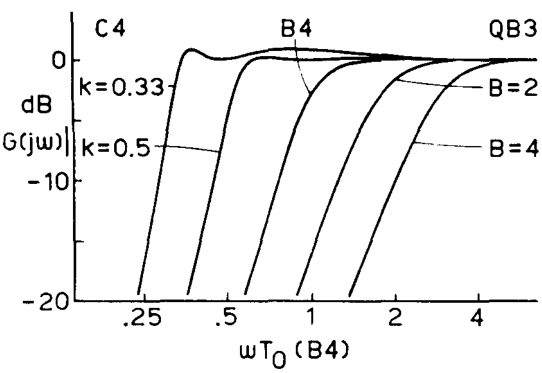

Fig. 5. Normalized response curves for B4 and selected C4 and QB3 alignments of vented-box loudspeaker system.

octave cutoff) high-pass filter function which may be expressed in the general form

$$G(s) = \frac{s^4 T_0^4}{s^4 T_0^4 + a_1 s^3 T_0^3 + a_2 s^2 T_0^2 + a_3 s T_0 + 1} \tag{20}$$

where T_0 is the nominal filter time constant and a_1, a_2, a_3 are coefficients which determine the behavior of the filter response.[1]

The behavior of Eq. (13) may be assessed by studying Eq. (20) and then using the relationships which make the corresponding terms of the two expressions identical. Using Eq. (11), these are

$$T_0 = (T_B T_S)^{1/2} = T_S / h^{1/2} \tag{21}$$

$$a_1 = \frac{Q_L + h Q_T}{h^{1/2} Q_L Q_T} \tag{22}$$

$$a_2 = \frac{h + (\alpha + 1 + h^2) Q_L Q_T}{h Q_L Q_T} \tag{23}$$

$$a_3 = \frac{h Q_L + Q_T}{h^{1/2} Q_L Q_T}. \tag{24}$$

Frequency Response

Alignment

The frequency response $|G(j\omega)|$ of Eq. (20) is examined in Appendix 1. Coefficient data are given for a variety of useful response characteristics which may be used to align the vented-box system.

Three very useful types of alignments are given by Thiele in [10]. These are the fourth-order Butterworth maximally flat alignment (B4), the fourth-order Chebyshev equal-ripple alignment (C4), and the alignment which Thiele has dubbed "quasi-third-order Butterworth" (QB3). Alternative alignments include the degenerated Chebyshev responses of Nomura [11] and the sub-Chebyshev responses of Thiele [14], although the latter provide less effective use of enclosure volume in relation to the efficiency and low-frequency cutoff obtained, i.e., a lower value of the efficiency constant described in Section 5.

[1] This normalization of the filter function follows the example of Thiele [10]. The relationships between this form of normalization and others, e.g., that used by Weinberg [18], including relative pole locations are given by Benson in [32, pp. 422-438 and Appendix 7].

Both the C4 and QB3 alignments provide a wide range of realizable response characteristics with gradually changing properties. Also, both as a limiting case coincide with the unique B4 alignment, so a completely continuous span of alignments is mathematically possible. A few of these alignments are illustrated in Fig. 5. The frequency scale of Fig. 5 is normalized to the nominal time constant of the B4 alignment; the other curves are plotted to the same scale but displaced horizontally for clarity. In this paper, the C4 alignments are specified by the value of k used by Thiele and defined in Appendix 1. The QB3 alignments are specified by the value of B defined in Appendix 1.

Inspection of Eqs. (21–24) reveals that the four mathematical variables needed to specify a given alignment, T_0, a_1, a_2, and a_3, are related to five independent system variables (or parameters), T_S, h, α, Q_L, and Q_T. This means that specification of a particular alignment does not correspond to a unique set of system parameters but may be obtained in a variety of ways. For any given alignment, one parameter may be assigned arbitrarily (within limits of realizability) and the rest may then be calculated.

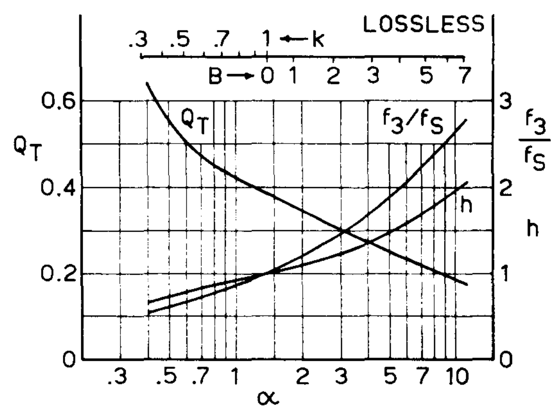

Fig. 6. Alignment chart for lossless vented-box systems.

A basic understanding of the behavior of the vented-box system is quickly obtained if the enclosure losses are ignored, i.e., Q_L is taken to be infinite. In this case, Eqs. (22–24) are simplified and all alignments become unique in terms of the system parameters. This is the process followed by Thiele in [10].

Fig. 6 is an alignment chart for systems with lossless enclosures based on the C4, B4, and QB3 alignments. The compliance ratio α is chosen as the primary independent variable and plotted as the abscissa of the figure. The corresponding values of k and B which specify the C4 and QB3 alignments are also given on the figure. Because each alignment is unique, every value of α corresponds to a specific alignment and requires specific values of the other system parameters to obtain the correct response. Thus the figure gives the values of Q_T and the tuning ratio $h = f_B/f_S$ required for each value of α, as well as the normalized cutoff frequency f_3/f_S at which the response is 3 dB down from its high-frequency asymptotic value.

Misalignment

The effect of an incorrectly adjusted parameter on the

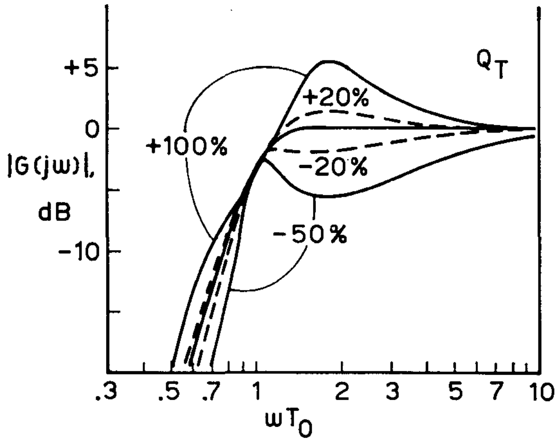

Fig. 7. Variations in frequency response of lossless B4-aligned vented-box system for misalignment of Q_T (from simulator).

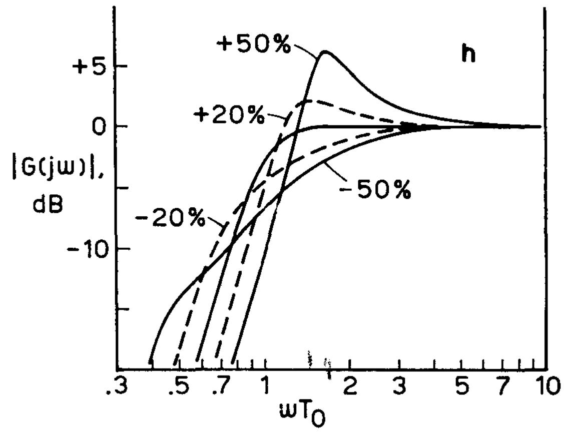

Fig. 8. Variations in frequency response of lossless B4-aligned vented-box system for misalignment of h (from simulator).

frequency response of a vented-box system is easily observed using the analog circuit simulator. Fig. 7 shows the variation produced in the response of a lossless system aligned for a B4 response by changes in the value of Q_T of $\pm 20\%$, -50%, and $+100\%$. This agrees exactly with [10, eqs. (42) and (43)] which indicate that the response at the frequencies f_L and f_H of the voice-coil impedance peaks is directly proportional to Q_T, while the response at f_B is independent of Q_T. Fig. 8 shows the variations produced in the same alignment by mistuning (changing the value of h) of $\pm 20\%$ and $\pm 50\%$.

Similar effects occur with other alignments. It is not difficult to see why the vented enclosure is sometimes scorned as a "boom box" when it is realized that the values of Q_T required are much lower than the majority of woofers provide [15, Table 13] and that a historical emphasis on unity tuning ratio regardless of compliance ratio often results in erroneously high tuning.

Alignment with Enclosure Losses

Using the approximation arrived at in Section 3, the parameter relationships required to provide a specified response in the presence of enclosure losses may be calculated as described in Appendix 1. Compared to lossless alignments, a particular response characteristic generally requires a larger value of Q_T and a smaller value of α.

Alignment charts for the C4, B4, and QB3 responses are presented in Figs. 9–13 for systems having enclosure losses corresponding to a Q_L of 20, 10, 7, 5, and 3, respectively. These values are representative of real enclosures, for which the most commonly measured values of Q_B are in the range of 5–10.

Transient Response

Keibs [8], [16] offered alignment solutions for what he considered to be the optimum transient response of a fourth-order filter. The same alignment parameters were later advocated by Novak [17]. The step responses of various fourth-order high-pass filter alignments are illustrated in Fig. 14. The alignments range from Chebyshev to sub-Chebyshev types and include the alignment recommended by Keibs.

The transient response of any minimum-phase network is of course directly related to the frequency response. For the vented-box system, the alignments which have more gradual rolloff also have less violent transient ringing. If transient response is considered important, then it would appear that the QB3 alignments are to be preferred over the B4 and C4 alignments. The SC4 alignments (Appendix 1) provide a further improvement in

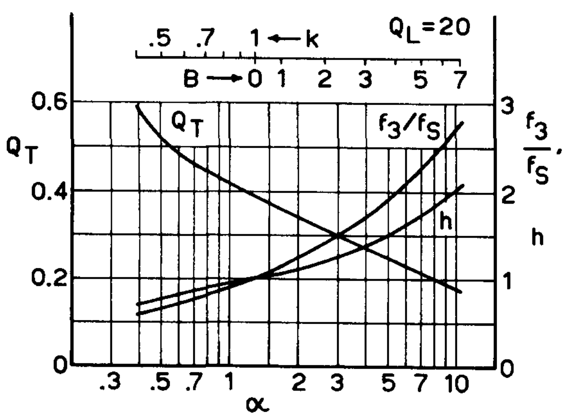

Fig. 9. Alignment chart for vented-box systems with $Q_B = Q_L = 20$.

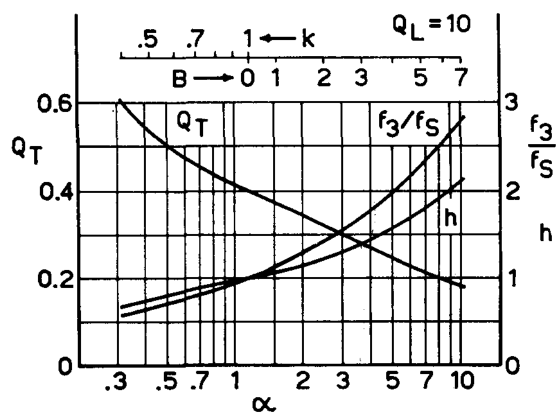

Fig. 10. Alignment chart for vented-box systems with $Q_B = Q_L = 10$.

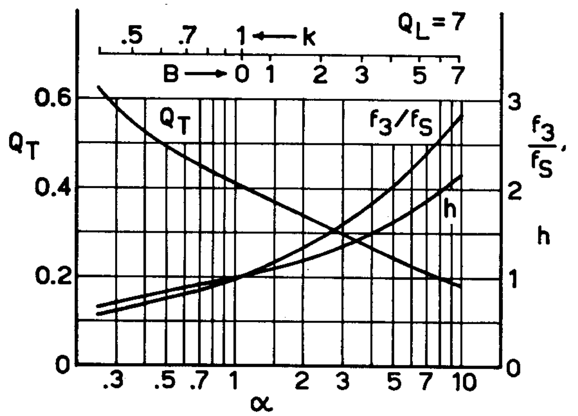

Fig. 11. Alignment chart for vented-box systems with $Q_B = Q_L = 7$.

transient response but have a less attractive frequency response.

Phase and Delay Response

Weinberg [18] shows how the conditions of maximal flatness or equal-ripple behavior may be imposed on any property of a response function, including phase response and group delay. The condition of maximally flat passband group delay is provided by the Bessel filter. The polynomial coefficients of the fourth-order Bessel filter are calculated in Appendix 1 from the pole locations given in [19].

General Response Realization

Any physically realizable minimum-phase fourth-order response characteristic which can be described in terms of the coefficients of Eq. (20) can be realized in a vented-box loudspeaker system. Using the method of Appendix 1, the coefficients may be processed into system alignment parameters which will produce the specified response.

5. EFFICIENCY

Reference Efficiency

The piston-range reference efficiency of a vented-box loudspeaker system is the reference efficiency of the system driver when the total air-load mass seen by the driver diaphragm is the same as that imposed by

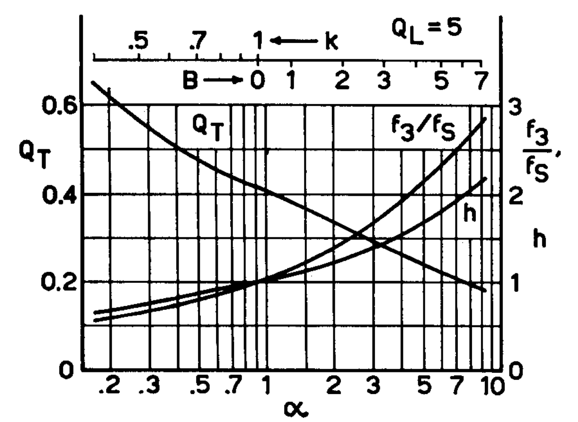

Fig. 12. Alignment chart for vented-box systems with $Q_B = Q_L = 5$.

the enclosure. Thus if the driver parameters are measured under or adjusted to correspond to this condition, the system reference efficiency η_0 is [12, eq. (32)]

$$\eta_0 = \frac{4\pi^2}{c^3} \cdot \frac{f_S{}^3 V_{AS}}{Q_{ES}}. \tag{25}$$

For SI units, the value of $4\pi^2/c^3$ is 9.64×10^{-7}.

Efficiency Factors

Eq. (25) may be written

$$\eta_0 = k_\eta f_3{}^3 V_B \tag{26}$$

where f_3 is the cutoff (half-power or -3 dB) frequency of the system, V_B is the net internal volume of the system enclosure, and $k\eta$ is an efficiency constant given by

$$k_\eta = \frac{4\pi^2}{c^3} \cdot \frac{V_{AS}}{V_B} \cdot \frac{f_S{}^3}{f_3{}^3} \cdot \frac{1}{Q_{ES}}. \tag{27}$$

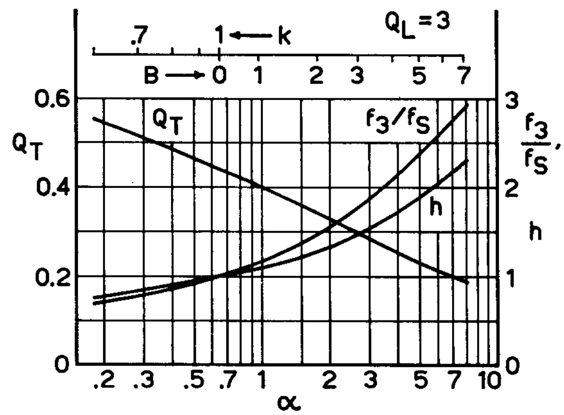

Fig. 13. Alignment chart for vented-box systems with $Q_B = Q_L = 3$.

The efficiency constant k_η may be separated into two factors, $k_{\eta(Q)}$ related to driver losses and $k_{\eta(G)}$ related to the response characteristic and enclosure losses. Thus,

$$k_\eta = k_{\eta(Q)} k_{\eta(G)} \tag{28}$$

where

$$k_{\eta(Q)} = Q_T/Q_{ES} \tag{29}$$

$$k_{\eta(G)} = \frac{4\pi^2}{c^3} \cdot \frac{V_{AS}}{V_B} \cdot \frac{f_S{}^3}{f_3{}^3} \cdot \frac{1}{Q_T}. \tag{30}$$

Driver Loss Factor

The value of Q_T for systems used with modern high-damping-factor amplifiers ($R_g = 0$) is equal to Q_{TS}, where [12, eq. (47)]

$$Q_{TS} = \frac{Q_{ES} Q_{MS}}{Q_{ES} + Q_{MS}}. \tag{31}$$

Eq. (29) then reduces to

$$k_{\eta(Q)} = Q_{TS}/Q_{ES} = 1 - Q_{TS}/Q_{MS}. \tag{32}$$

This expression has a maximum value of unity which is approached only when mechanical driver losses are negligible (Q_{MS} infinite) and all required damping is

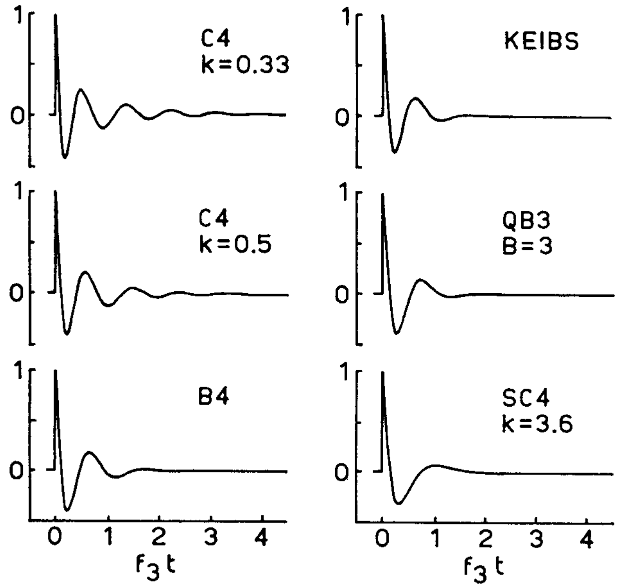

Fig. 14. Normalized step response of vented-box loudspeaker system (from simulator).

provided by electromagnetic coupling ($Q_{ES} = Q_{TS}$).

The value of $k_{\eta(Q)}$ for typical vented-box system drivers is in the range of 0.8–0.95.

System Response Factor

Normally, vented enclosures contain only a small amount of damping material used as a lining. Under these conditions [3, p. 129],

$$C_{AB} = V_B/\rho_0 c^2 \tag{33}$$

and, using Eqs. (9) and (10), Eq. (30) can be written in terms of the system parameters as

$$k_{\eta(G)} = \frac{4\pi^2}{c^3} \cdot \frac{\alpha}{Q_T(f_3/f_S)^3}. \tag{34}$$

The relationships between α, Q_T, and f_3/f_S for the C4–B4–QB3 alignments have already been calculated and plotted in Figs. 6 and 9–13. Thus the value of $k_{\eta(Q)}$ for any of these alignments can also be calculated. Fig. 15 is a plot of the value of $k_{\eta(G)}$ as a function of α for several values of Q_L. For reference, the location

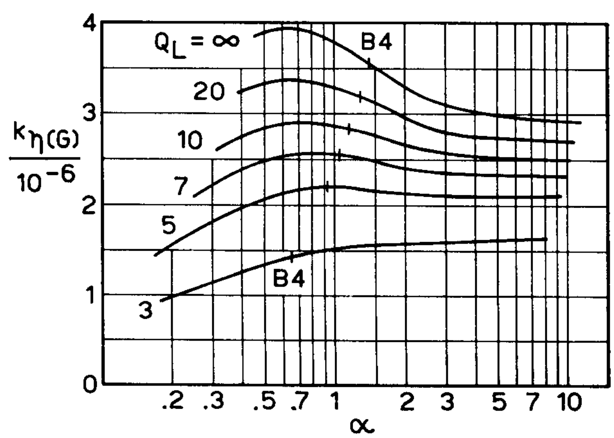

Fig. 15. Response factor $k_{\eta(G)}$ of efficiency constant for vented-box loudspeaker system as a function of α (system compliance ratio) for several values of enclosure Q.

of the B4 alignment is indicated on each curve by a short vertical bar.

It is clear that enclosure losses significantly reduce the value of $k_{\eta(G)}$ for a correctly aligned system. The maximum possible value of $k_{\eta(G)}$ is 3.9×10^{-6} and occurs when the enclosure losses are negligible and the system compliance ratio is adjusted to about 0.6. This is a $k = 0.5$ C4 alignment which has a ripple of about 0.2 dB.

Maximum Reference Efficiency, Cutoff Frequency, and Enclosure Volume

Taking the maximum theoretical values of $k_{\eta(Q)}$ and $k_{\eta(G)}$, the maximum reference efficiency $\eta_{0(\max)}$ that could be obtained from a lossless vented-box system for specified values of f_3 and V_B is, from Eqs. (26) and (28),

$$\eta_{0(\max)} = 3.9 \times 10^{-6} f_3^3 V_B \tag{35}$$

with f_3 in Hz and V_B in m³. This relationship is illustrated in Fig. 16, with V_B (given here in cubic decimeters: 1 dm³ = 1 liter = 10^{-3} m³) plotted against f_3 for various values of $\eta_{0(\max)}$ expressed in percent.

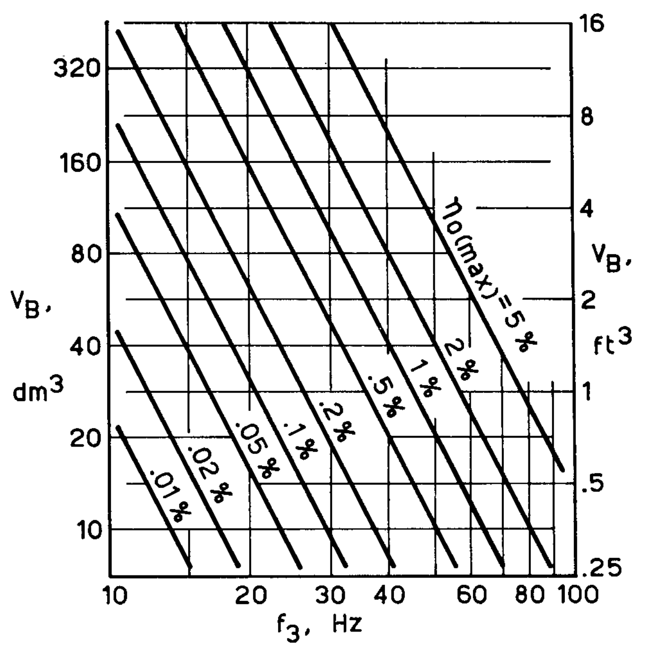

Fig. 16. Relationship between cutoff frequency, enclosure volume, and maximum reference efficiency for vented-box loudspeaker system.

Fig. 16 represents the physical efficiency–cutoff frequency–volume limitation of vented-box system design. A practical system having given values of f_3 and V_B must always have an actual reference efficiency lower than the corresponding value of $\eta_{0(\max)}$ given by Fig. 16. Similarly, a system of specified efficiency and volume must have a cutoff frequency higher than that indicated by Fig. 16, and so on.

Actual vented-box systems have an efficiency lower than the maximum given by Eq. (35) because of driver mechanical losses, enclosure losses, and the use of alignments other than that which gives maximum efficiency for a given value of Q_L. Typical practical efficiencies are 40–50% (2–3 dB) lower than the theoretical maximum given by Eq. (35) or Fig. 16. For most systems, the driver parameters can be measured and the reference efficiency calculated directly from Eq. (25).

The physical limitation imposed by Eq. (35) or Fig. 16 may be overcome in a sense by the use of amplifier assistance, i.e., networks which raise the gain of the amplifier in the cutoff region of the system [10], [20]. While the overall response of the complete system is thus extended, there is no change in the driver-enclosure efficiency in the cutoff region. The amplifier must deliver more power, and the driver must dissipate this power.

REFERENCES—PART I

[1] A. L. Thuras, "Sound Translating Device," U.S. Patent No. 1,869,178, application Aug. 15, 1930, patented July 26, 1932.

[2] B. N. Locanthi, "Application of Electric Circuit Analogies to Loudspeaker Design Problems," *IRE Trans. Audio,* vol. PGA-6, p. 15 (Mar. 1952); republished in *J. Audio Eng. Soc.,* vol. 19, p. 778 (Oct. 1971).

[3] L. L. Beranek, *Acoustics* (McGraw-Hill, New York, 1954).

[4] F. J. van Leeuwen, "De Basreflexstraler in de Akoestiek," *Tijdschrift Nederlands Radiogenootschap,* vol. 21, p. 195 (Sept. 1956).

[5] E. de Boer, "Acoustic Interaction in Vented Loudspeaker Enclosures," *J. Acoust. Soc. Amer.* (Letter) vol. 31, p. 246 (Feb. 1959).

[6] R. H. Lyon, "On the Low-Frequency Radiation Load of a Bass-Reflex Speaker," *J. Acoust. Soc. Amer.* (Letter), vol. 29, p. 654 (May 1957).

[7] J. F. Novak, "Performance of Enclosures for Low-Resonance High-Compliance Loudspeakers," *IRE Trans. Audio,* vol. AU-7, p. 5 (Jan./Feb. 1959); also *J. Audio Eng. Soc.,* vol. 7, p. 29 (Jan. 1959).

[8] L. Keibs, "The Physical Conditions for Optimum Bass Reflex Cabinets," *J. Audio Eng. Soc.,* vol. 8, p. 258 (Oct. 1960).

[9] E. de Boer, "Synthesis of Bass-Reflex Loudspeaker Enclosures," *Acustica,* vol. 11, p. 1 (1961).

[10] A. N. Thiele, "Loudspeakers in Vented Boxes," *Proc. IREE (Australia),* vol. 22, p. 487 (Aug. 1961); republished in *J. Audio Eng. Soc.,* vol. 19, p. 382 (May 1971) and p. 471 (June 1971).

[11] Y. Nomura, "An Analysis of Design Conditions of a Bass-Reflex Loudspeaker Enclosure for Flat Response," *Electron. Commun. Japan,* vol. 52-A, no. 10, p. 1 (1969).

[12] R. H. Small, "Direct-Radiator Loudspeaker System Analysis," *IEEE Trans. Audio Electroacoust.,* vol. AU-19, p. 269 (Dec. 1971); republished in *J. Audio Eng. Soc.,* vol. 20, p. 383 (June 1972).

[13] D. E. L. Shorter, "Loudspeaker Cabinet Design," *Wireless World,* vol. 56, p. 382 (Nov. 1950), and p. 436 (Dec. 1950).

[14] A. N. Thiele, "Filters with Variable Cut-off Frequencies," *Proc. IREE (Australia),* vol. 26, p. 284 (Sept. 1965).

[15] J. R. Ashley and M. D. Swan, "Improved Measurement of Loudspeaker Driver Parameters," presented at the 40th Convention of the Audio Engineering Society, Los Angeles (Apr. 1971), Preprint 803.

[16] B. C. Reith, "Bass-Reflex Enclosures," *Wireless World,* (Letter), vol. 73, p. 38 (Jan. 1967).

[17] J. F. Novak, "Designing a Ducted-Port Bass-Reflex Enclosure," *Electron. World,* vol. 75, p. 25 (Jan. 1966).

[18] L. Weinberg, *Network Analysis and Synthesis* (McGraw-Hill, New York, 1962), ch. 11.

[19] R. M. Golden and J. F. Kaiser, "Root and Delay Parameters for Normalized Bessel and Butterworth Low-Pass Transfer Functions," *IEEE Trans. Audio Electroacoust.,* vol. AU-19, p. 64 (Mar. 1971).

[20] A. N. Thiele, "Equalisers for Loudspeakers," presented at the 12th National Convention of the IREE (Australia), (May 1969).

[32] J. E. Benson, "Theory and Design of Loudspeaker Enclosures, Part 3—Introduction to Synthesis of Vented Systems," *A.W.A. Tech. Rev.,* vol. 14, p. 369 (Nov. 1972).

Editor's Note: Dr. Small's biography appeared in the December issue.